A non-linear multiscale chemo-mechanical model describing the delayed evolution of concrete structures in marine environments

Marinelle El-Khoury, Frederic Grondin, Emmanuel Rozière, Rachid Cortas, Fadi Hage Chehade

Mechanics & Industry **24**, 25 (2023)
© M. El-Khoury et al., Published by EDP Sciences 2023
https://doi.org/10.1051/meca/2023023

History of matter: from its raw state to its end of life
Prof. Amine Ammar (Guest Editor)

Mechanics & Industry

Available online at:
www.mechanics-industry.org

REGULAR ARTICLE

OPEN ACCESS

A non-linear multiscale chemo-mechanical model describing the delayed evolution of concrete structures in marine environments

Marinelle El-Khoury[1,2,*], Frédéric Grondin[1], Emmanuel Roziere[1], Rachid Cortas[3], and Fadi Hage Chehade[2]

[1] Nantes Université, Ecole Centrale Nantes, CNRS, GeM, UMR 6183, 44000 Nantes, France
[2] Centre de Modélisation, Ecole Doctorale des Sciences et Technologie, Université Libanaise, Liban
[3] Centre de Recherches Scientifiques en Ingénierie (CRSI), Université Libanaise, Beyrouth, Liban

Received: 21 December 2022 / Accepted: 3 July 2023

Abstract. The failure of offshore structures is a major issue as they lead to economic, environmental, and social disasters. Assessing the durability and long-term behavior of these structures subjected to chemical and mechanical degradation is subsequently critical. The analysis of these coupled phenomena induced by seawater attack and mechanical loading is complex and requires the development of innovative measurement systems and modelling strategies. Thus, multiscale protocols, starting from the microscopic scale of the cement paste, seems relevant for the characterization of the chemo-mechanical behavior of offshore structures. Therefore, the competition between protective layers' formations and harmful effects of seawater ions has been coupled with the creep phenomenon.

Keywords: Cement / chemo-mechanical / degradation / multi-scale / seawater

1 Introduction

Controlling the environmental conditions of concrete structures is almost impossible. Therefore, it should be considered as a given parameter in a durability study. While implementing durability assessment protocols, it is essential to get as close as possible to the real conditions to obtain representative results.

Seawater exposure is critical due to its complex composition and the multiple phenomena induced by the seawater ions [1,2]. Previous studies have focused on sulfate attack characterization [3] and on chloride diffusion [4]. At equivalent sulfate concentration levels, seawater exhibits distinct characteristics compared to sulfate attack [5]. Given the competition between the protective and expansive effects [6,7], it seems interesting to represent seawater as a combination of all the anions and cations present in the seawater during its reformulation in the laboratory.

The chemo-mechanical coupling between calcium leaching and mechanical damage of cementitious materials has been studied by [8–11]. It shows a strong coupling between calcium leaching and mechanical behavior: as leaching increases, a loss of stiffness and strength has been experimentally observed [11]. Leached concrete becomes more ductile during chemical degradation [11,12]. The coupling between creep and leaching of concrete has been studied in [12–14]. It has been observed that the deformation in the combined test accelerates and reaches tertiary creep [13]. This demonstrates the effect of long time loading combined with leaching.

There has been limited research conducted on the coupling between chemical degradation and mechanical effects, particularly in terms of modeling and experimental procedures. It is also noteworthy that no study has associated the creep phenomenon to the seawater attack.

To study the chemo-mechanical coupling, a new multiscale numerical and experimental approach will be presented in this study. The paper focuses on the combined effects of hydration associated with seawater attack, and their effects on the creep and mechanical performance of offshore structures by considering all the ions present in seawater.

2 Multiscale chemo-mechanical protocol

2.1 Multiscale modelling

Distinguishing the effects of the ions present in seawater and their effects on the microstructure and the overall mechanical behavior of the structure is experimentally exhaustive. Moreover, the attack of seawater is slow, so that to reach advanced degrees of degradation, it takes several years. Thus, the use of reliable numerical models is

* e-mail: marinelle.el-khoury@ec-nantes.fr

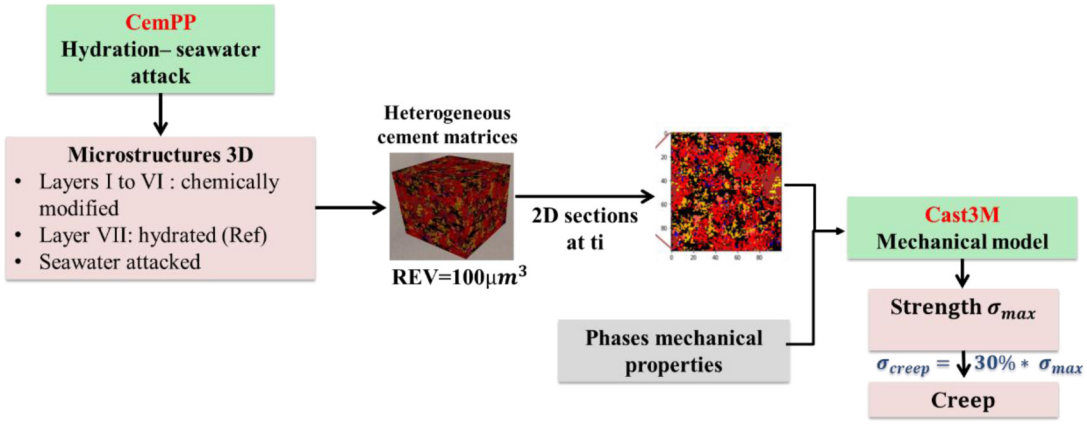

Fig. 1. Multiscale chemo mechanical modeling.

essential to model the effect of each ion on the microstructure and to represent the chemo-mechanical phenomena over long periods.

The cement paste represents a heterogeneous material composed of multiple phases such as anhydrous cement particles and hydration products, such as calcium hydroxide (CH), calcium silicate hydrate (C-S-H), ettringite, etc. The hydration of the heterogeneous cement paste is modeled using CemPP v 0.2 [15], based on the hydration code CEMHYD3D v3 developed at NIST [16]. CemPP is a modified version of CEMHYD3D originally developed to simulate the cement hydration process and understand the kinetics and the potential of the self-healing phenomenon [15].

At the mortar scale, the material is assumed to be made of two continuous media: the cement paste, considered in this case as homogeneous, and the sand particles. The simulation of the chemo-mechanical coupling proposed in this work considers a mechanical calculation on a material whose microstructure has evolved chemically and where damage and viscoelastic behavior are coupled.

For this purpose, two codes have been associated:

– CemPP [15], for the simulation of hydration and chemical reactions at the cement paste scale (the model combines hydration and seawater attack),
– The finite element code Cast3M for the simulation of the mechanical behavior, loss or gain of elastic properties defining consequently the mechanical strength of the structure (mechanical damage model based on [17,18] (Eqs. (1) and (2)), as well as creep using 4 chains of Kelvin Voight (Eq. (3)).

The cement paste represents a heterogeneous material composed of anhydrous cement and hydration products. Mechanical properties of the cement hydrate phases have been gathered from literature and summarized in the work of [19]. The damage model adopted for the cementitious phases is the one developed by Fichant et al. [17,18]. A strong assumption was made in the creep model: All phases except C-S-H have a negligible viscoelastic behavior compared to C-S-H [20–23]. The total stress σ is calculated from the effective stress (Eq. (1)), and the viscoelastic strain tensor ε^v is calculated according to the creep compliance J(t) using 4 chains of Kelvin–Voight (Eqs. (2) and (3)):

$$\sigma = (1\text{–D})\ C^0 : \varepsilon^e = (1 - D)\ C^0 : (\varepsilon^T - \varepsilon^v) \quad (1)$$

$$\varepsilon^v = J(t) \otimes \sigma \quad (2)$$

$$J(t) = \sum_{i=1}^{n} \frac{1}{\kappa_i}\left(1 - e^{-\frac{\kappa_i}{\eta_i}t}\right) \quad (3)$$

where $\tau_i = \eta_i / k_i$ represent the characteristic times of the Kelvin–Voigt chains: τ_1=0.1 day, τ_2= 1 day, τ_3=10 days, and τ_4=100 days, and k_i the elementary phase stiffness [20–22].

After defining the mechanical behavior of the cement paste, a homogenization method was designed to assess the properties of the mortar. At the mortar scale, the creep-damage model requires the following input parameters: Young's modulus, Poisson's coefficient, strength, rigidity, density, fracture energy and creep coefficients (Elementary rigidity). The start of cement exposure is 3 days. The algorithm used at a time of calculation "t_i" is summarized in Figure 1, where σ_{max} is the strength of the microstructure at time t_i and σ_{creep} is the creep applied on the microstructure at the same time t_i.

First of all, using the chemical reactions defined in CEMHYD3D, the simulation of hydration is performed by cycles of dissolution, diffusion, and precipitation.

Secondly, since the chemical action of seawater must be described as one of many reactions taking place simultaneously [24], and since the chemical reaction time has been assumed to be much faster than diffusion, seawater attack results in layers corresponding to the different fronts of dissolution/precipitation. The characteristic size of the microstructure being very small, a total replacement of the cement phases by their reaction product is adopted. Each layer represents ionic/chemical attack and product formation. To understand fully the effect of each phase formed or transformed on the mechanical behavior of the structure, each layer is simulated separately as a material under hydration-chemical reaction coupling. Then, the

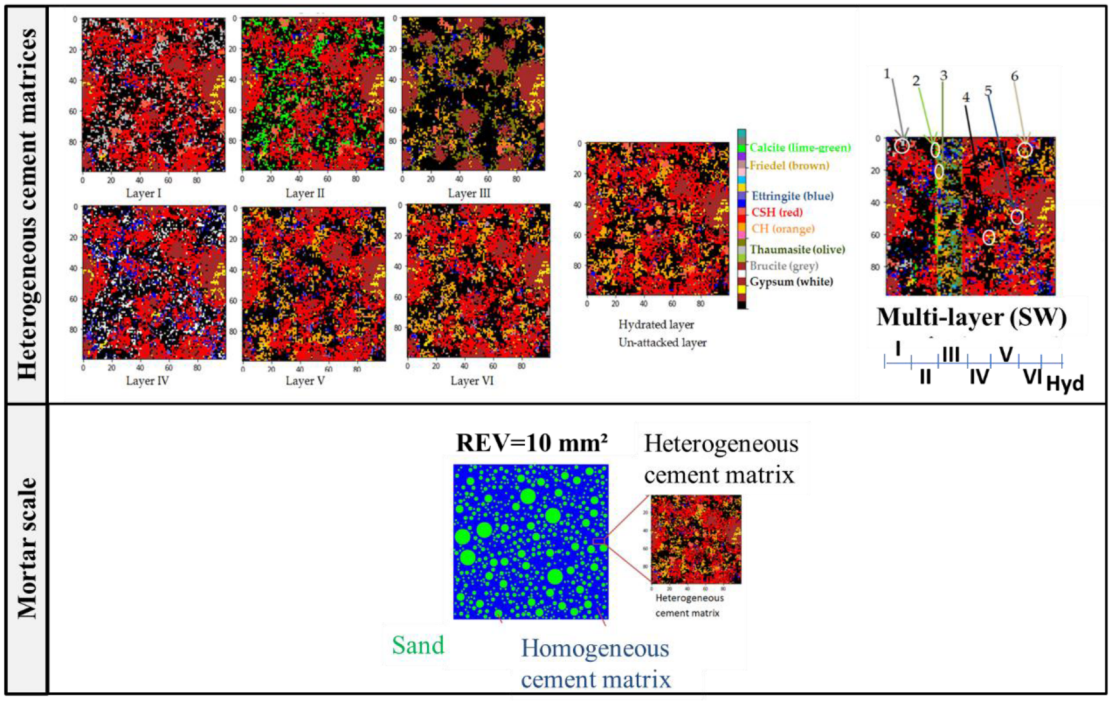

Fig. 2. The heterogeneous chemically modified cement matrices simulated at the age of 28 days and the mortar REV.

multilayer modified microstructure named "SW" is compared to the hydrated intact one named "Ref" (Fig. 2). The simulation of the hydration-seawater attack coupling process was carried out on 100 μm^3 cement paste using CemPP and 10 mm^2 for mortar using Cast3M. The color variation between the modified layers and the hydrated unattacked layer highlights the phase changes in the microstructure.

Layer I is a Brucite-rich layer (Grey color) :

$$Mg^{2+} + Ca(OH)_2 \rightarrow Mg(OH)_2 + Ca^{2+}. \quad (4)$$

Layer II models the $CaCO_3$ rich layer (lime-green color):

$$Ca(OH)_2 + CO_2 \rightarrow CaCO_3 + H_2O. \quad (5)$$

Layer III represents the reaction of CSH from sources of sulfate and carbonate [25] and the formation of thaumasite (olive color):

$$3CaO.2SiO_2.3H_2O + 2(CaSO_4.2H_2O) + CaCO_3 + CO_2 + 23H_2O \rightarrow 2Ca_3\left[Si(OH)_6\right](CO_3)(SO_4).12H_2O. \quad (6)$$

The presence of sulfate can lead to the formation of gypsum (layer IV, white color) and ettringite (layer V, blue color) via the following equations:

$$Mg^{2+} + SO_4^{2-} + Ca(OH)_2 \rightarrow CaSO_4 + Mg(OH)_2 \quad (7)$$

$$Ca^{2+} + SO_4^{2-} + C_3A + 32H_2O \rightarrow C_3A.3CaSO_4.32H_2O. \quad (8)$$

The diffusion of chloride ions can lead to the formation of Friedel's salt:

$$C_3A + Ca(OH)_2 + 2Cl^- + 10H_2O \rightarrow C_3A.CaCl_2.10H_2O + 2OH^-. \quad (9)$$

Friedel

Layer VI represents a Friedel salt rich layer (brown color).

Finally, the combination of all these layers is supposed to form a heterogeneous cement matrix modified by seawater attack [22].

2.2 Experimental procedure

2.2.1 Experimental program

To validate the model, experiments were performed at both scales of mortar and paste. The experimental characterization presents the originality of considering all the ions present in the seawater solution. Mortar cylinders have been prepared using a water to cement (W/C) ratio of 0.6 and ordinary Portland cement (OPC). Its composition and properties are presented in Table 1.

Cement paste cylinders were prepared with W/C = 0.5. At the age of 3 days, the specimens were immersed in tap water ("Ref.") and in a laboratory reconstituted seawater ("SW"). For diffusion acceleration purposes a W/C = 0.6 and salinity of 70 g/L (equivalent to the double of reference seawater [26]) were considered. Epoxy resin layers were also applied at the two surface ends to ensure 2D diffusion.

Table 1. Composition and properties of used Portland cement.

C_3S	60.0%
C_2S	16.3%
C_3A	7.7%
C_4AF	10.5%
Gypsum	3.5%
Other constituents	2.0%
Density (10^3 kg/m^3)	3.16
Blaine (m^2/kg)	400

The experimental protocol illustrated in Figure 3 allows analyzing the effect of seawater attack on cementitious materials at the chemo-mechanical scale. This analysis was carried out at the macroscopic scale (variation of mass, volume and length) by including mechanical criteria (estimation of strength and stiffness). At the microscopic scale, the characterization allows to identify the formed and transformed phases using cement paste samples. To include long time loadings in the study, a new creep rig was designed and implemented (Fig. 3).

2.2.2 Mechanical evaluation

The compressive strength of three plain mortar samples was determined at each characterization age (1, 2, 7, 28, and 145 days), and the average compressive strength was calculated. During the test, the load was applied at a rate of 0.5 MPa/s until failure. The static elastic modulus was determined using an extensometer and LVDT sensors on two samples at the same ages mentioned earlier. The specimens were loaded and unloaded up to a load equal to 30% of their strength to measure the elastic modulus.

Creep was applied on hollow samples immerged in seawater and tap water. The constant load was equal to 30% of the sample's strength determined at the age of loading.

2.2.3 Macroscopic evaluation

The degradation of the samples was assessed during the exposure period by measuring the changes in length and weight on a weekly basis. This evolution was monitored on three hollow samples and three plain samples immersed in seawater (SW) and six samples (3 hollow and 3 plain) in tap water (Ref).

2.2.4 Microscopical phase's changes evaluation

Scanning electron microscopy (SEM) and energy-dispersive spectroscopy (EDS) were performed to visualize and analyze the polished cement paste samples immersed in seawater and those immersed in tap water. Prior to SEM observations, the cylindrical specimens underwent transverse cutting. Then they were embedded in a low-modulus epoxy resin and subjected to a polishing process. These preparation steps were carried out to ensure optimal conditions for SEM analysis.

Thermogravimetric analysis (TGA) was carried out on cement paste samples crushed into powders and analyzed in a dry nitrogen atmosphere using a Netzsch SRA449 F3 apparatus. The samples were heated from 20 to 900 °C at a constant rate. This analysis helped identify and quantify the phases resulting from seawater attack. The samples were extracted from the surface and center of paste specimens.

Qualitative identification of crystalline phases was carried out using an Aeris X-ray diffraction (XRD) instrument, and the analysis covered cement paste samples crushed into powders and sieved at 80 μm. Similar to TGA, XRD analysis was performed on the surface and the center of the cement paste samples. The scan was performed between 7° and 70° using a Cu Kα source ($\lambda1 = 1.540$ Å and $\lambda2 = 1.544$ Å) with a 0.38 mm slit.

3 Results and discussions

Figure 4 shows the evolution of product thickness deposited at the mortars surface. This evolution was determined by calculating the average on three samples. Figure 5 shows the evolutions of phases formed at the paste surface sample determined using TGA technique.

It can be seen that the samples recorded a positive thickness indicating that new products have been formed at the surface. The thickness deposited at the surface of hollow cylinders was higher than that of plain cylinders. This can be explained by the higher exposure surface of hollow cylinders. Thickness evolutions are linear with respect to the square root of time, highlighting the ions diffusions following Fick's law. The diffusion of ions from the surface and their reaction with the cement hydration products induced the formation of this deposited layer. The phases formed at the sample's surface were identified using TGA (Fig. 5).

Results show the formation of brucite ($Mg(OH)_2$) and calcium carbonate ($CaCO_3$) and the consumption of calcium hydroxide ($Ca(OH)_2$). The results highlight the reactions presented in equations (4) and (5).

Calcium carbonate was also found on the surface of control samples (Ref.). In these samples, calcium carbonate formed rapidly during the first 30 days and then gradually decreased or stabilized. Previous studies on the effects of groundwater on cement-based materials have shown that calcium carbonate can form [27].

Figure 6 summarizes the phases identified using XRD analysis at the surface and the center of control and SW samples after one year of exposure.

Figure 7 shows the chloride profiles for control and SW samples identified using energy dispersive spectroscopy analysis.

Brucite, located at $2\theta = 37.966°$ on XRD graph could only be observed on the surface of samples immersed in seawater. This is in agreement with the results obtained using TGA analysis (Fig. 5). Similarly, Friedel's salt was

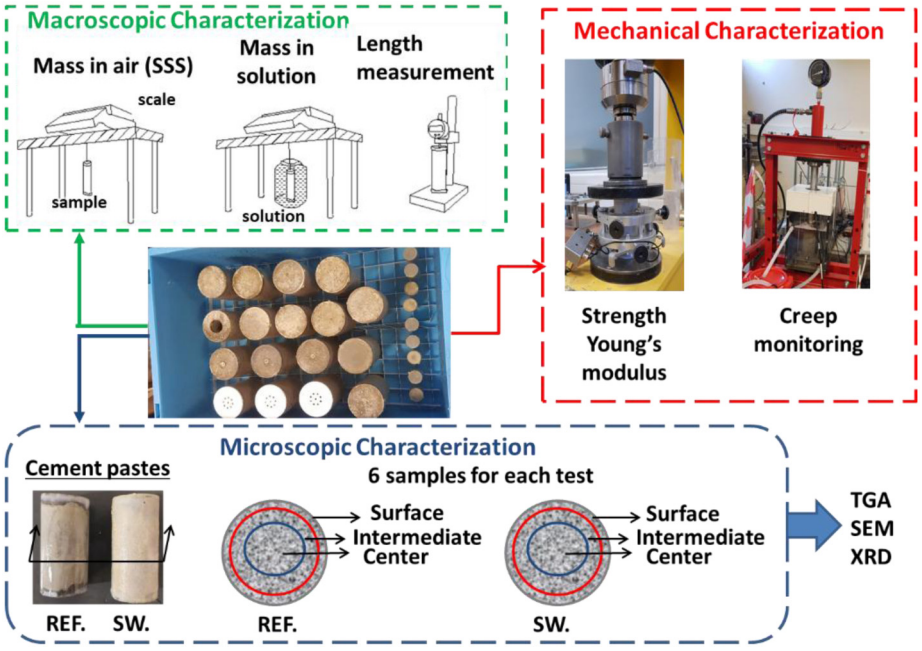

Fig. 3. Multiscale experimental chemo-mechanical characterization. REF: control specimens. SW: specimens in seawater.

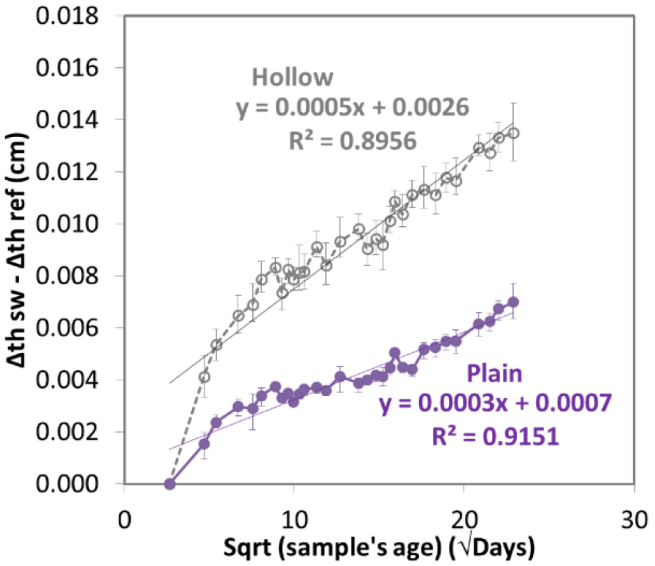

Fig. 4. Evolution of material thickness deposited at the sample surface.

identified in the SW samples at peak $2\theta = 11.193°$ confirming the reaction of chloride ions with cement hydrates. This result highlights the reaction presented in equation (9).

Unlike brucite, Friedel's salt could be detected in the center and on the surface of the samples immersed in the marine solutions, which could confirm the diffusion of chloride ions from the surface to the center of the samples. This diffusion was detected in Figure 7 using EDS analysis.

The expected gypsum peak at ($2\theta = 11.438°$ and $2\theta = 20.731°$) could only be observed at the surface of samples immersed in a marine solution at an advanced age of immersion (one year). Aragonite and vaterite formed on the surface of the exposed samples, confirming the greater amount of $CaCO_3$ observed in the TGA analysis on the surface of samples exposed to seawater (Fig. 5). Calcite was observed in both control and exposed samples. The ettringite peak appeared in both cases of immersion. This does not indicate that its formation is favored in seawater. Sulfate attack generally induces expansion by crystallization pressures due to ettringite formation. The longitudinal expansion remained very small during the experiments [7]. Thus, sulfate attack had less influence due to the chloride penetration [5] and the formation of Friedel's salt.

According to the chemical reactions actually taking place in the specimens, the microstructures have been numerically built in CEMPP.

Figure 8 illustrates the distribution of C-S-H content in each layer at the age of 28 days, as well as the changes in creep compliance over a period of 3 years. The observed data reveals a significant initial increase in creep compliance during the initial days of loading, followed by a subsequent asymptotic trend. This behavior suggests a gradual but diminishing viscoelastic displacement rate over time. The simulations also highlight the effects of the chemically modified layers (layer I to VI) on the overall behavior of the seawater attacked microstructure.

Figure 9 shows the maximum creep compliance (J_{max}) recorded after 3 years of loading as a function of the proportion of C-S-H present in the cement pastes microstructure. Figures 8 and 9 allow concluding that the ettringite-rich layer (layer V) recorded the highest creep and the gypsum-rich layer (layer IV) recorded the

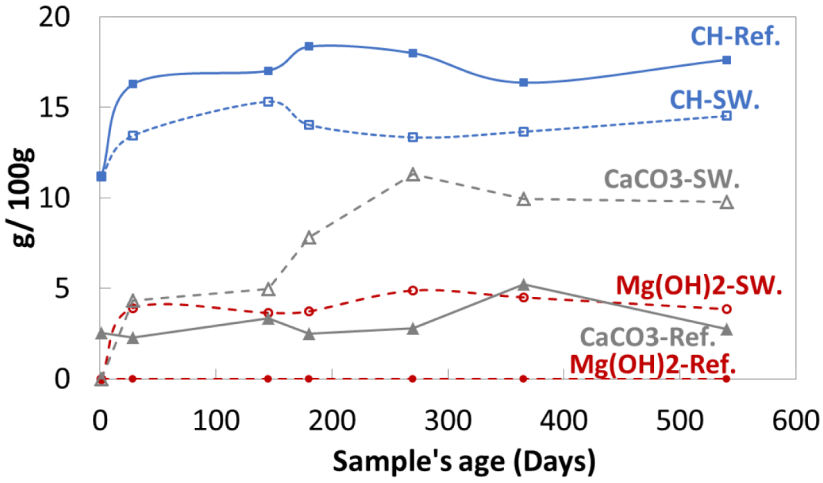

Fig. 5. Phases identification at the sample's surface using TGA.

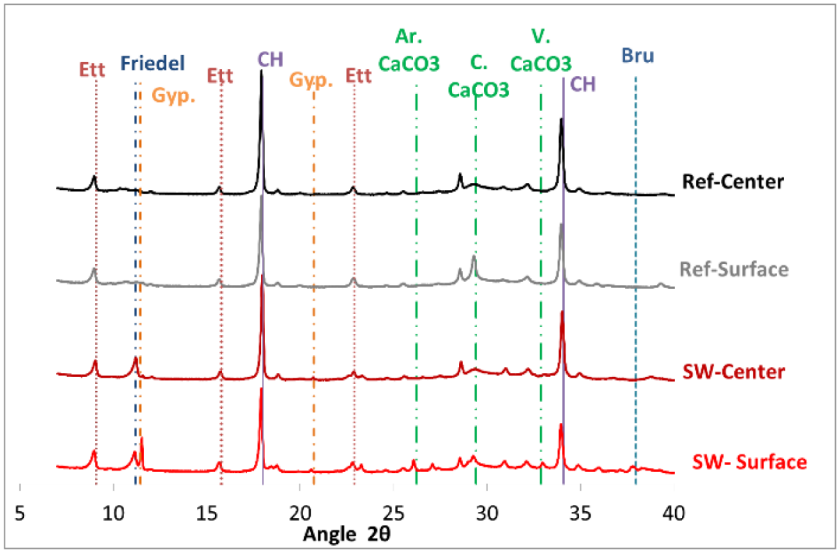

Fig. 6. XRD phases identification after one year exposure for control paste (Ref) and pastes exposed to seawater (SW) after one year.

lowest creep, regardless of the age of loading. It should be noted that the expansive character of ettringite (crystallization pressures) is not taken into account by the model, as the experimental results obtained did not show any macroscopic expansion and damage after two years of follow-up [7].

This graph joins the simulations performed at the following loading ages: 7 days, 14 days, 28 days, 2 months, 4 months, and 6 months (one point per layer and per loading age). Figure 10 shows an agreement between the numerically calculated specific displacements due to creep applied at age 28 days and those experimentally monitored for control and attacked hollow mortars.

The attacked multilayer cement microstructure (SW) recorded a lower creep than the control sample. This can be explained by the lower amount of C-S-H present in the seawater attacked microstructure especially due to the presence of layer III simulating the C-S-H consumption and which presented a negligible creep (Fig. 8). The adopted model restores the difference between the mechanical behaviors of the chemically modified layers even with the same rate of C-S-H in these microstructures. Globally, this is consistent with the mechanical model hypothesis, which considers that C-S-H is the main phase involved in creep.

In Figure 10, it can be seen that creep of mortars increase quickly in the first days of load application and that the creep displacements for reference mortars are slightly lower than attacked mortar. This highlights that the effect of seawater attack-creep coupling is not predominant at long term (after 3 days of loading). This compensation between positive and negative effects can be explained with the difference in the behavior of layers (Figs. 8 and 9).

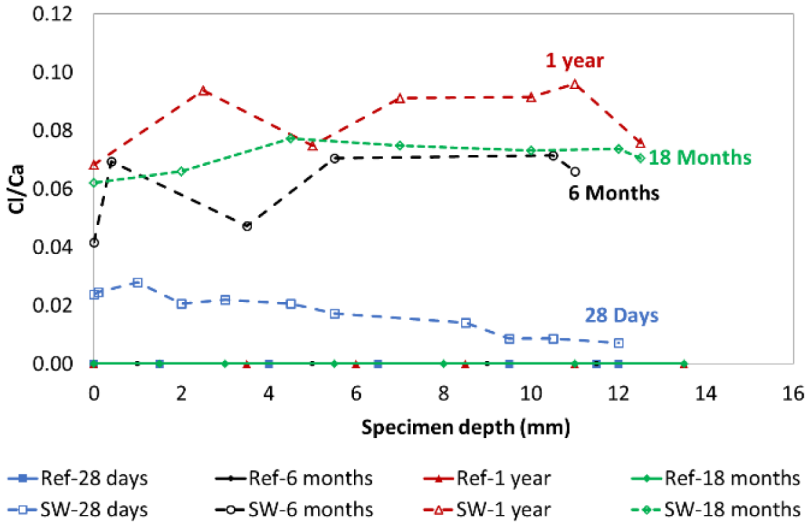

Fig. 7. Chloride profiles identified using energy dispersive spectroscopy analysis.

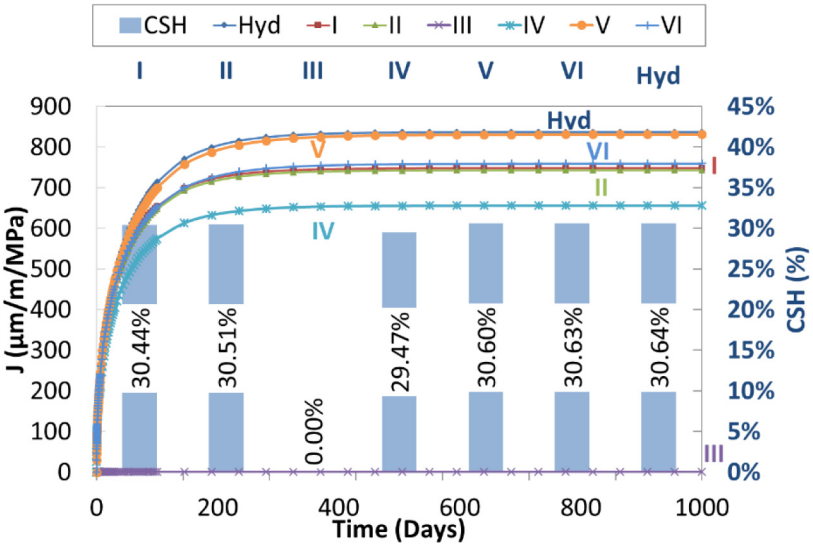

Fig. 8. Chemically modified layers: creep compliance and CSH content present when loading at the age of 28 days [22].

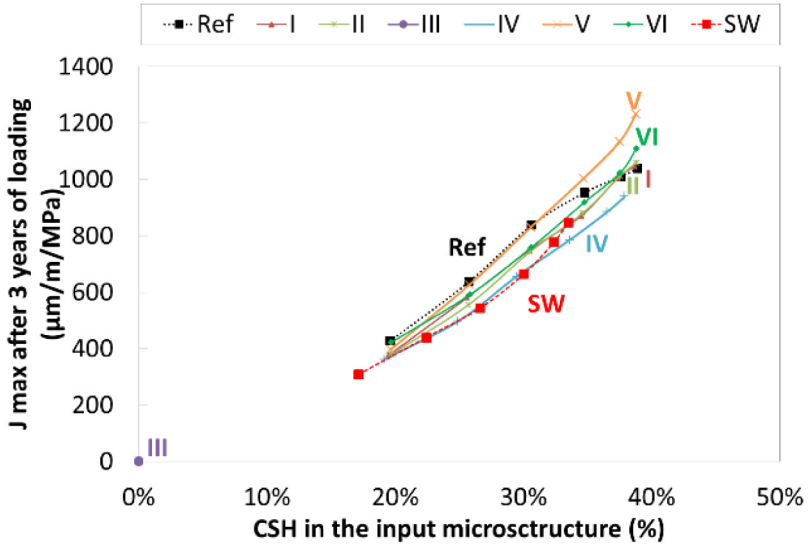

Fig. 9. Creep compliance and CSH contents of chemically modified layers of cement paste.

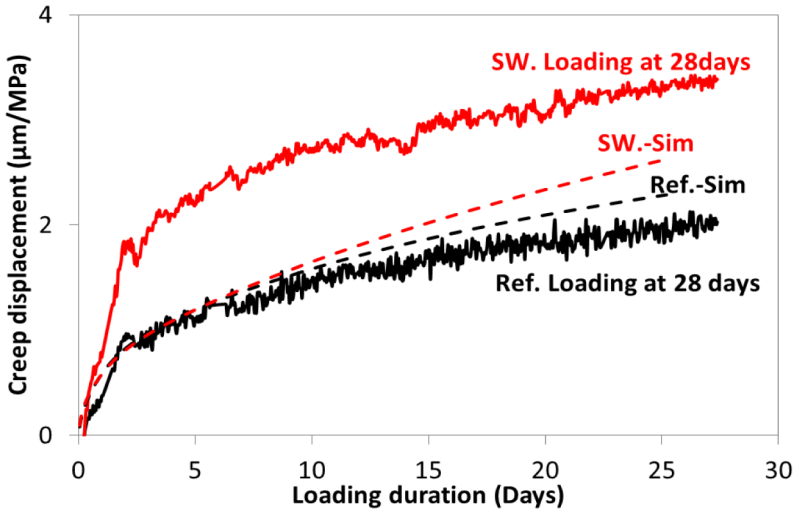

Fig. 10. Creep displacement of mortars: Experimental vs. numerical approach.

4 Conclusions

A numerical multiscale model has been developed to analyze the mechanical creep behavior of cement-based materials in seawater. A new experimental test has been performed for the same goal. The mechanical creep behavior of attacked samples remained equal to that of the reference samples, even though significant microstructural changes and rapid penetration of chloride ions were observed at the microscopic level. Experimental analysis added explanation on the type of products formed during attacks. Mortar and cement paste cylinders were characterized by the highest amount of products formed at the surface as a result of exposure to seawater. The material deposited at the surface of specimens was identified by microscopic characterization methods (SEM/EDS, XRD, and TGA). The protective effect of brucite and calcium carbonate surface layers could be detected. Their linear evolution as a function of the square root of time follows Fick's law. Sulfate attack in seawater was not predominant, with minor expansion and ettringite formation, and the pore blocking effect of brucite and calcium carbonate near the surface could have slowed down ionic diffusion in the cement matrix. Similarly, this could be attributed to the presence of chloride ions that mitigate sulfate attack. By considering these chemical effects in the model, simulations of creep for cement pastes and mortars have been performed. The model was used to explain the creep evolution due to a competition between the dissolution-formation of different phases in cement paste and the loading. This model can now be used for the simulation of concrete structures.

Funding

This work has received funding from the Lebanese University, Ecole Centrale of Nantes, and the Carnot Marine Engineering Research for Sustainable, Safe and Smart Seas Institute.

Acknowledgments. The authors would like to acknowledge the French Association of Mechanics (AFM) for selecting their contribution to CFM 2022.

References

[1] K. De Weerdt, H. Justnes, M.R. Geiker, Changes in the phase assemblage of concrete exposed to sea water, Cement Concrete Composites **47**, 53–63 (2014)
[2] E. Guillon, Durabilité des matériaux cimentaires: modélisation de l'influence des équilibres physico-chimiques sur la microstructure et les propriétés mécaniques résiduelles, École Normale Supérieure de Cachan, 2004
[3] R. Ragoug et al., Durability of cement pastes exposed to external sulfate attack and leaching: physical and chemical aspects, Cement Concrete Res. **116**, 134–145 (2019)
[4] M. Zhang, J. Chen, Y. Lv, D. Wang, J. Ye, Study on the expansion of concrete under attack of sulfate and sulfate − chloride ions, Constr. Build. Mater, **39**, 26–32 (2013)
[5] M. Santhanam, M. Cohen, J. Olek, Differentiating seawater and groundwater sulfate attack in Portland cement mortars, Cement Concrete Res. **36**, 2132–2137 (2006)
[6] M. El-Khoury, F. Grondin, E. Rozière, R. Cortas, F. Hage Chehade, Chemo-mechanical coupling model of off-shore concrete structures, Acad. J. Civil Eng. **39**, 39–42 (2021)
[7] M. El-Khoury, E. Roziere, F. Grondin, R. Cortas, F. Hage Chehade, Experimental evaluation of the effect of cement type and seawater salinity on concrete offshore structures, Constr. Build. Mater. **322**, 126471 (2022)
[8] D. Kuhl, F. Bangert, G. Meschke, Coupled chemo-mechanical deterioration of cementitious materials. Part I. Modeling, Int. J. Solids Struct. **41**, 15–40 (2004)
[9] D. Kuhl, F. Bangert, G. Meschke, Coupled chemo-mechanical deterioration of cementitious materials. Part II. Numerical methods and simulations, Int. J. Solids Struct. **41**, 41–67 (2004)
[10] V.H. Nguyen, B. Nedjar, J.M. Torrenti, Chemo-mechanical coupling behaviour of leached concrete. Part II. Modelling, Nuclear Eng. Des. **237**, 2090–2097 (2007)

[11] V.H. Nguyen, H. Colina, J.M. Torrenti, C. Boulay, B. Nedjar, Chemo-mechanical coupling behaviour of leached concrete. Part I. Experimental results, Nuclear Eng. Des. **237**, 2083–2089 (2007)
[12] L. Lacarrière, A. Sellier, X. Bourbon, Concrete mechanical behaviour and calcium leaching weak coupling, Rev. Eur. Génie Civil **10**, 1147–1175 (2006)
[13] J.M. Torrenti, V.H. Nguyen, H. Colina, F. Le Maou, F. Benboudjema, F. Deleruyelle, Coupling between leaching and creep of concrete, Cement Concrete Res. **38**, 816–821 (2008)
[14] O. Bernard, F.J. Ulm, J.T. Germaine, Volume and deviator creep of calcium-leached cement-based materials, Cement Concrete Res. **33**, 1127–1136 (2003)
[15] B. Hilloulin, D. Hilloulin, F. Grondin, A. Loukili, N. De Belie, Mechanical regains due to self-healing in cementitious materials: experimental measurements and micro-mechanical model, Cement Concrete Res. **80**, 21–32 (2016)
[16] D.P. Bentz, A three-dimensional cement hydration and microstructure program. I. Hydration rate, heat of hydration, and chemical shrinkage, NISTIR **5756** (1995)
[17] S. Fichant, C. La Borderie, G. Pijaudier-cabot, Isotropic and anisotropic descriptions of damage in concrete structures, Mech. Cohesive Frictional Mater. **4**, 339–359 (1999)
[18] S. Fichant, G. Pijaudier-cabot, C. La Borderie, Continuum damage modelling: approximation of crack induced anisotropy, Mech. Res. Commun. **24**, 109–114 (1997)
[19] A. Rhardane, S.Y. Alam, F. Grondin, The role of surface micro-cracks in cementitious materials responsible for the Pickett effect, Mech. Time-Depend. Mater. (2021), doi: 10.1007/s11043-021-09509-w
[20] C. Youssef Namnoum, B. Hilloulin, F. Grondin, A. Loukili, Modelling of creep effect on a healed crack in cementitious materials, in: 10th International Conference on Fracture Mechanics of Concrete and Concrete Structures FraMCoS-X., 2019, pp. 1–7
[21] A. Rhardane, Élaboration d'une approche micromécanique pour modéliser l'endommagement des matériaux cimentaires sous fluage et cycles de gel-dégel, Ecole Centrale de Nantes, 2018.
[22] M. El-khoury, F. Grondin, B. Hilloulin, E. Roziere, R. Cortas, F.H. Chehade, Creep analysis of cementitious materials in seawater using a poro-chemo-mechanical model, Mar. Struct. J. **90** (2023), doi: 10.1016/j.marstruc.2023.103431
[23] A. Rhardane, F. Grondin, S.Y. Alam, Development of a micro-mechanical model for the determination of damage properties of cement pastes, Constr. Build. Mater. **261**, 120514 (2020)
[24] M. Eglinton, Resistance of concrete to destructive agencies, in: P.C. Hewlett (Ed.), Lea's Chemistry of Cement and Concrete – Fourth Edition, Elsevier Ltd. 1998, pp. 299–342
[25] M. Santhanam, M.D. Cohen, J. Olek, Effects of gypsum formation on the performance of cement mortars during external sulfate attack, Cement Concrete Res. **33**, 325–332 (2003)
[26] F.J. Millero, R. Feistel, D.G. Wright, T.J. McDougall, The composition of standard seawater and the definition of the reference-composition salinity scale, Deep-Sea Res. Part I: Oceanogr. Res. Pap. **55**, 50–72 (2008)
[27] A. Gauthier, Approche expérimentale et modélisation de la lixiviation des ouvrages de traitement d ' eau potable en béton exposés à des eaux agressives, Ecole Centrale de Nantes, 2020

Cite this article as: M. El-Khoury, F. Grondin, E. Roziere, R. Cortas, F. Hage Chehade, A non-linear multiscale chemo-mechanical model describing the delayed evolution of concrete structures in marine environments, Mechanics & Industry **24**,25 (2023)